Test of a Hadronic Interaction Model by a Multidimensional Analysis of Lateral and Longitudinal Air-Shower Observables at KASCADE

F. Badea[1,a], T. Antoni[1], W.D. Apel[2], K. Bekk[2], A. Bercuci[2,a], H. Blümer[1,2], H. Bozdog[2], I.M. Brancus[3], C. Büttner[1], A. Chilingarian[4], K. Daumiller[1], P. Doll[2], R. Engel[2], J. Engler[2], F. Feßler[2], H.J. Gils[2], R. Glasstetter[1,b] A. Haungs[2], D. Heck[2], J.R. Hörandel[1], A. Iwan[5], K-H. Kampert[1,2,b], H.O. Klages[2], G. Maier[2], H.J. Mathes[2], H.J. Mayer[2], J. Milke[2], M. Müller[2], R. Obenland[2], J. Oehlschläger[2], S. Ostapchenko[1,c], M. Petcu[3], H. Rebel[2], M. Risse[2], M. Roth[1], G. Schatz[2], H. Schieler[2], J. Scholz[2], T. Thouw[2], H. Ulrich[2], J. van Buren[2], A. Vardanyan[4], A. Weindl[2], J. Wochele[2], J. Zabierowski[5]

(1) Institut für Exp. Kernphysik, Universität Karlsruhe, 76021 Karlsruhe, Germany
(2) Institut für Kernphysik, Forschungszentrum Karlsruhe, 76021 Karlsruhe, Germany
(3) National Institute of Physics and Nuclear Engineering, 7690 Bucharest, Romania
(4) Cosmic Ray Division, Yerevan Physics Institute, Yerevan 36, Armenia
(5) Soltan Institute for Nuclear Studies, 90950 Lodz, Poland
[a] *on leave of absence from (3)*
[b] *now at: Universität Wuppertal, 42097 Wuppertal, Germany*
[c] *on leave of absence from Moscow State University, 119899 Moscow, Russia*

Abstract

The multi-detector experiment KASCADE enables simultaneous observations of parameters describing the lateral and longitudinal development of Extensive Air Showers. The present analysis is focused on Field Array and Muon Tracking detectors of KASCADE. The Field Array (FA) provides the numbers of electrons and muons in the shower and the Muon Tracking Detector (MTD) measures angles-of-incidence of muons which are related to the longitudinal development of EAS. An identical two step deconvolution method (on primary mass using a Bayesian approach and on primary energy) is performed to calculate the primary mass and energy of cosmic rays using the correlation of FA observables only and by adding MTD observables. The consistency of the CORSIKA/QGSJET simulation code in describing the correlation between lateral and longitudinal developments of the shower is studied by comparing the results obtained from the two sets of observables.

1. FA and MTD Observables

The KASCADE experiment [2] allows extensive air-shower measurements in the primary energy range around the *knee*. The FA consists of shielded and

pp. 25–28

unshielded scintillation detectors measuring the electromagnetic and muonic components with 5 MeV and 230 MeV energy thresholds, respectively. FA provides the basic information about the arrival direction (θ, ϕ) and core position as well as the numbers of muons (N_μ) and electrons (i.e. *shower size* N_e) of the observed EAS. Additionally, the so-called *truncated number of muons* (N_μ^{tr}) is derived, i.e. number of muons between 40 and 200 m distance from the shower core. At KASCADE N_μ^{tr} is used as an approximate primary energy estimator. The Muon Tracking Detector [6] detects muons with 0.8 GeV energy threshold. The MTD consists of 16 towers of 3 horizontal modules (limited streamer tubes) each. There is a strong correlation between the longitudinal development of the muonic component and the radial angles [4] of the muon incidence with respect to the shower axis. For a multiplicity $n \geq 1$ of muons reconstructed from 3-hit-tracks at the 128 m^2 sensitive area of the MTD, two observables of interest are calculated on an event-by-event basis: *mean distance* $(r_{\mu mean})$ of the MTD muons to the shower axis and the *median radial angle* $(\rho_{0.50})$, i.e. the median value [1] of the radial angle distribution.

2. Experimental and Simulated Data

An amount of 40 million EAS events observed with KASCADE has been analysed. The experimental sample shrunk to 600 000 showers after applying the following cuts: $\theta < 40°$, distance between shower core and FA center below 90 m, $3.4 < log_{10} N_\mu^{tr} < 5.4$ and at least one muon track in the MTD. Simulations have been performed with the code CORSIKA (version 5.62) [8] with a full and detailed simulation of the detector response. QGSJET (version 1998) model [9] has been used as generator for high-energy hadronic interactions and GHEISHA [7] for interactions below $E_{lab} = 80$ GeV. The electromagnetic part is treated by the EGS4 program [10]. Around 500 000 showers have been simulated for each of the 4 primaries (proton H, Helium He, Oxygen O and Iron Fe) in the primary energy range from 10^{14} up to 10^{18} eV with a spectral index $\gamma = -2.0$.

3. Primary Mass Discrimination

A non-parametric multivariate analysis has been used for separating different primary masses [5]. The *true-classification* P_{ii} and *misclassification* P_{ij} $(i \neq j)$ probabilities have been calculated for a classification procedure based on Bayes decision rule $(i, j \in \{H, (He), C, Fe\})$. Fig. 1 shows the variation with $log_{10} N_\mu^{tr}$ of the geometrical mean values of the true-classification probabilities for 3 zenith angle ranges and for the cases of classification in 3 and 4 primary masses. A systematic improvement for the primary mass discrimination has been obtained by adding the MTD observables $\{r_{\mu mean}, \rho_{0.50}\}$ to the basic correlation $\{N_\mu^{tr}, N_e\}$ provided by the FA.

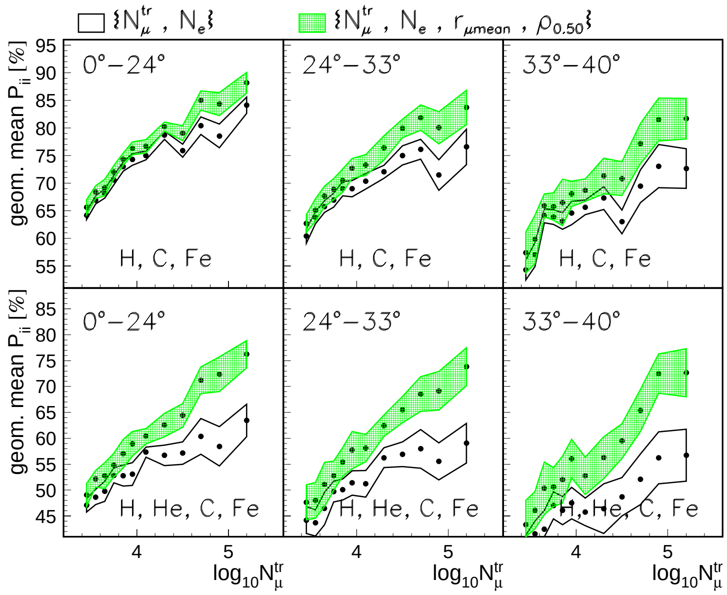

Fig. 1. The dependence of the geometrical mean values of P_{ii} on $log_{10}N_\mu^{tr}$.

4. Test of the Monte Carlo Simulation Procedures

The reconstruction of the primary mass composition depends on the high-energy hadronic interaction model generating the Monte Carlo simulations. An opportunity to test the internal consistency of a model is to derive the primary mass composition(s) by the analysis of different sets of observables. The test is based on primary mass compositions reconstructed by FA observables only and by taking into account the correlation of FA&MTD observables which have to be identical after applying all correction factors. The true-classification and misclassification probabilities, deduced for the 3 zenith angle ranges and for 12 (non-equal) bins of $log_{10}N_\mu^{tr}$, have been used for the reconstruction of the *experimental* sample compositions. Fig. 2A shows the results for 2 zenith angle ranges and 3 primary masses, for FA observables only (upper panel) and for FA&MTD correlation (lower panel). The *statistical* errors shown in all figures have been calculated using a bootstrap method [5]. A good agreement between the sample mass compositions reconstructed for the two sets of observables was found. But differences of the results are revealed by comparing various zenith angle ranges, which can be explained by different acceptance efficiencies for the different primaries [3]. Using simulations, the acceptance matrices have been calculated for each zenith angle range and primary type. These matrices contain for each primary energy bin the fraction of the primaries contributing to different N_μ^{tr} bins. A second deconvolution, on primary energy, has been done by combining the experimental sample compositions (Fig. 2A) with these acceptance matrices. The results of the deconvolution are displayed in Fig. 2B as primary mass compositions (up to a normalisation constant) unified over all 3 zenith angle ranges. The primary mass

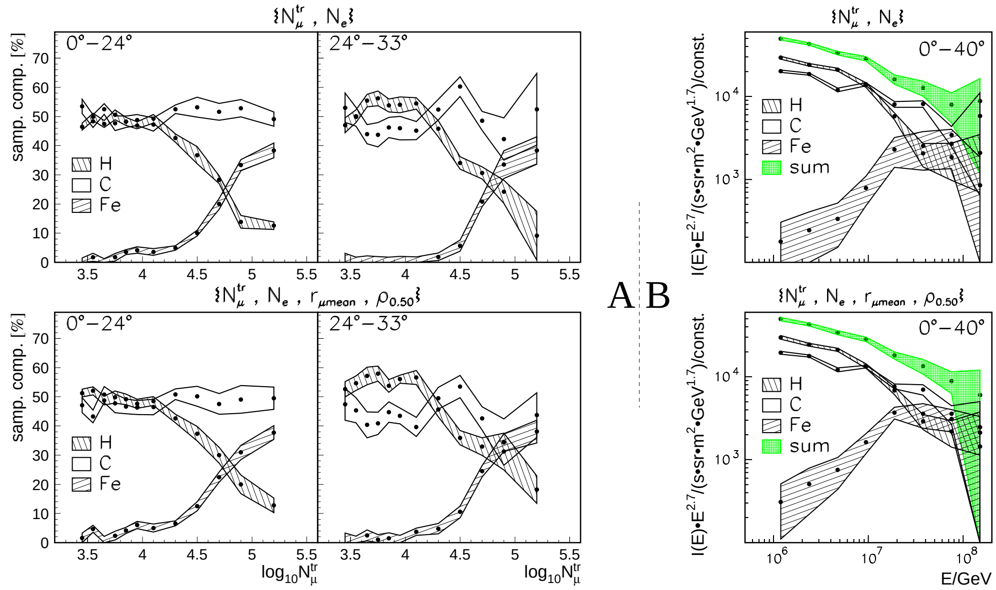

Fig. 2. Experimental sample compositions (A) and primary mass composition (B).

compositions based on the two sets of observables look very similar within the limits of the statistical uncertainties.

5. Conclusions

An improvement of the primary mass discrimination has been found by adding the muon angles-of-incidence to the Field Array information of shower size and number of muons. The behaviours of the total primary spectrum and primary mass composition seen by the present analysis confirm earlier published KASCADE results. The invariance of the primary mass composition with respect to the two sets of observables (FA only and FA&MTD) proves the consistency of the CORSIKA/QGSJET simulation code in describing the threefold correlation shower size - number of muons - longitudinal muon development, but is not a proof on the description of the absolute numbers of muons and electrons in the model.

1. Antoni T. et al. - KASCADE Collaboration 2001, Astropart. Phys. 15, 149
2. Antoni T. et al. - KASCADE Collaboration, submitted to Nucl. Instr. Meth. A
3. Antoni T. et al. - KASCADE Collaboration 2003, Astropart. Phys. 18, 319
4. Büttner C. et al. - KASCADE Collaboration 2003, these Proceedings
5. Chilingarian A.A. 1989, Comp. Phys. Comm. 54, 381
6. Doll P. et al. 2002, Nucl. Instr. Meth. A 488, 517
7. Fesefeldt H. 1985, Report PITHA - 85/02, RWTH Aachen
8. Heck D. et al. 1998, Report FZKA 6019, Forschungszentrum Karlsruhe
9. Kalmykov N.N. et al. 1997, Nucl. Phys. B (Proc. Suppl.) 52B, 17
10. Nelson W.R. et al. 1985, Report SLAC-265, Stanford Lin. Acc. Center